24 Jun 1994

The Response of Dispersion-Strengthened Copper Alloys to High Fluence Neutron Irradiation at 415ºC

Danny J. Edwards

Joseph William Newkirk
Missouri University of Science and Technology, jnewkirk@mst.edu

Frank A. Garner

Margaret L. Hamilton

et. al. For a complete list of authors, see https://scholarsmine.mst.edu/matsci_eng_facwork/2159

2

Conf-920673--9

PNL-SA--19956

DE92 019434

THE RESPONSE OF DISPERSION-STRENGTHENED COPPER ALLOYS TO HIGH FLUENCE NEUTRON IRRADIATION AT 415°C

D. J. Edwards
J. W. Newkirk
F. A. Garner
M. L. Hamilton
A. Nadkarny
P. Samal

June 1992

Presented at the
ASTM 16th Annual Symposium on Effects of
Radiation on Materials
June 22-24, 1992
Denver, Colorado

Work supported by
the U.S. Department of Energy
under Contract DE-AC06-76RLO 1830

Pacific Northwest Laboratory
Richland, Washington 99352

The Response of Dispersion-Strengthened Copper Alloys To High Fluence Neutron Irradiation at 415°C

D.J. Edwards[1], J.W. Newkirk[1], F.A. Garner[2]
M.L. Hamilton[2], A. Nadkarny[3], and P. Samal[3]

[1] University of Missouri, Rolla, MO, USA
[2] Pacific Northwest Laboratory, Richland, WA, USA
[3] SCM Metal Products, Bradfordwoods, PA, USA

ABSTRACT

Various oxide-dispersion-strengthened copper alloys have been irradiated to 150 dpa at 415°C in the Fast Flux Test Facility (FFTF). The Al_2O_3-strengthened GlidCop™ alloys, followed closely by a HfO_2-strengthened alloy, displayed the best swelling resistance, electrical conductivity, and tensile properties. The conductivity of the HfO_2-strengthened alloy reached a plateau at the higher levels of irradiation, instead of exhibiting the steady decrease in conductivity observed in the other alloys. A high initial oxygen content resulted in significantly higher swelling for a series of castable oxide-dispersion-strengthened alloys, while a Cr_2O_3-strengthened alloy showed poor resistance to radiation.

INTRODUCTION

One of the most crucial components of the International Thermonuclear Experimental Reactor (ITER) is the divertor plate assembly, which will be subjected to a high heat flux (~25 MW/m^2) from the charged particles and thermal energy that escape the plasma, and radiation damage from the 14 MeV neutrons and charged particles [1-5]. As a consequence of this severe irradiation environment, the divertor plate assembly must utilize structural materials that can maintain high strength and high thermal conductivity throughout its lifetime.

The high thermal conductivity requirement leads to the consideration of pure copper and its alloys. Pure copper, however, is not generally considered

a structural material due to its low strength and low softening temperature. In addition, irradiation experiments [6-11] in the Fast Flux Test Facility (FFTF) have demonstrated that pure copper has little resistance to void swelling, which dramatically decreases the electrical conductivity. The thermal conductivity will also decrease since the two conductivities are directly proportional to each other. The FFTF experiments also revealed that oxide-dispersion-strengthened (ODS) copper alloys demonstrated the most promising behavior after irradiation to ~100 dpa, exhibiting excellent swelling resistance and good retention of electrical conductivity and strength. Transmutation of the copper produced enough nickel and zinc to lower the conductivity, an effect which becomes more noticeable as the fluence increases [12,13].

On the basis of electrical conductivity and yield strength, the GlidCop™ alloys are considered a prime candidate material for current divertor plate designs, possibly being used for the heat sink and perhaps the tubing that carries the coolant. Typical designs, shown in Fig. 1, call either for carbon fiber composite (CFC) tiles to be brazed onto the plasma-facing surface of the copper heat sink, or for the divertor block to be made entirely of CFC with a metal coolant tube, possibly fabricated from dispersion-strengthened copper. The tiles act as an armor to prevent the thermal erosion of the copper and thus reduce the contamination of the plasma by high Z elements, and also allow higher temperatures to be obtained at the divertor surface without melting the copper [2,5]. Some of the problems associated with using copper alloys for the divertor include brazing difficulties due to mismatches in the thermal expansion coefficients of the copper and CFC's, and melting of the copper during a loss of cooling accident [2].

In this report the results of density measurements, tensile tests, fractography, and electrical conductivity measurements (used to estimate thermal conductivity) are presented for various dispersion-strengthened copper alloys irradiated to 104 and 150 dpa at 415°C in FFTF. Although these displacement levels are considerably higher than anticipated for ITER applications (~10 dpa), understanding the irradiation effects on the materials at these high displacement levels may be useful for commercial reactor applications.

EXPERIMENTAL

The copper alloys irradiated in FFTF are listed in Table 1 along with their compositions and thermomechanical treatments. Although the three alloy classes are all dispersion-strengthened systems, each class was produced by a different method. The GlidCop™ alloys are produced by SCM Metal Products using an internal oxidation technique [14], which yields a very fine, uniform dispersion of Al_2O_3 particles, imparting high strength and yet allowing good electrical conductivity. The CuAl15 alloy contains ≤200 ppm boron, which was used as a deoxidant.

The second class of alloys studied were two mechanically alloyed copper alloys incorporating either Cr_2O_3 or HfO_2 as the strengthening particles. Dr. N. Grant at the Massachusetts Institute of Technology supplied these alloys. The alloys were produced using powder metallurgy techniques involving the mixing of pure copper powder and the metal oxide powder and then extruding the final powder at 700°C using a 16:1 extrusion ratio.

The third class of alloys represented an attempt by Technical Research Associates, Inc. to produce a castable, oxide-dispersion-strengthened alloy. As will be shown later, this effort proved unsuccessful for an unexpected reason. The alloy was produced by adding oxide particles (coated with copper by a proprietary chemical coprecipitation method) to a melt of magnesium-bearing oxygen-free high conductivity (OFHC) copper, and then casting the melt. The ODS-1 and ODS-2 alloys have the same composition but were produced from different melts. The ODS-3 and ODS-4 alloys contain more magnesium than the two previous alloys, but the ODS-3 alloy uses ZrO_2 as the oxide dispersion instead of the Al_2O_3 used in the other three alloys.

Both transmission electron microscopy (TEM) disks and miniature tensile specimens [15, 16] were punched from sheet stock of the various materials; only TEM disks were punched from the ODS-2 stock. Tensile specimens of CuAl25 and ODS-1 were also fabricated from strips of 0.25 mm thick sheet that had been cut and then joined together by laser welding. The tensile specimens were punched from the welded sheet so that the weld was centered in the gage length. TEM disks were also punched from the weld regions.

Density measurements were obtained at room temperature from TEM disks, using an immersion density technique accurate to ±0.16% density change. Electrical conductivity measurements were made at room temperature on both miniature tensile specimens and TEM disks using a four-point, probe DC potential drop method described by Anderson and coworkers [9]. The dimensions of the miniature tensile specimens are given in Fig. 2. Conductivity measurements on both types of specimens were in good agreement with each other. Tensile tests were performed after the conductivity measurements were completed, using a miniature tensile testing apparatus developed specifically

for this specimen geometry [15,16]. Tensile tests were performed at room temperature with a free-running crosshead speed of 0.0025 mm s^{-1}, which yields an initial strain rate of 4.8×10^{-4} s^{-1}.

Table 1 ODS Copper Alloys Irradiated in FFTF at ~415°C

ALLOY	COMPOSITION (WT%)	THERMO-MECHANICAL PROCESSING
GlidCop[IM] Alloys*		
CuAl15 + boron	0.15% Al as Al_2O_3, <200 ppm residual boron	Annealed, 900°C/0.5 hr/ air cooled (AC)
CuAl20	0.20% Al as Al_2O_3	20% cold worked (CW)
CuAl25	0.25% Al as Al_2O_3	50% CW
CuAl25 WELD	Same, laser welded	50% CW
Mechanically Alloyed Copper**		
Cu-HfO_2	1.1 % Hf as HfO_2	20% CW, 450°C/0.5 hr/AC
Cu-Cr_2O_3	3.5% Cr as Cr_2O_3	20% CW, 450°C/0.5 hr/AC
Castable Copper Alloys***		
ODS-1	0.25% Mg, 1% Al_2O_3	40% CW
ODS-1 WELD	Same, laser welded	40% CW
ODS-2	0.25% Mg, 1% Al_2O_3	40% CW
ODS-3	0.50% Mg, 1% ZrO_2	40% CW
ODS-4	0.50% Mg, 1% Al_2O_3	40% CW

* Produced by SCM Metal Products
** Supplied by Prof. N. Grant at Massachusetts Institute of Technology
*** Produced by Technical Research Associates, Inc., Salt Lake City, Utah

Fracture surfaces were examined in both a JEOL 840 scanning electron microscope and a JEOL JSM 35C. Oxidation of the surfaces can occur quickly and obscure detail at magnifications higher than 1000x, so specimens were loaded into one of the microscopes immediately after being tested.

RESULTS

Castable ODS Alloys

Swelling data for the castable ODS alloys are presented in Fig. 3 along with data on pure copper for comparison. As a group, all four alloys exhibit poor swelling resistance, roughly paralleling the swelling behavior of pure copper, although significant differences are apparent for the various ODS alloys. The ODS-4 alloy exhibits considerably less swelling than pure copper and the other three alloys, however. The swelling resistance of the ZrO_2-strengthened ODS-3 alloy is the lowest. Laser welding obviously has an additional detrimental effect on the swelling of the ODS-1 alloy because the welded ODS-1 material displays the most swelling, greater than that of pure copper.

Figure 4 shows that the electrical conductivity of the castable ODS alloys lies within a common band that steadily decreases with increasing irradiation. Notice that the conductivity for the ODS-3 alloy lies near the bottom of the band, which is not unexpected since it exhibits the greatest swelling of the four alloys. Conductivity for the laser welded ODS-1 alloy was not obtained because of surface irregularities caused by the weld zone developing considerably more swelling than that of the surrounding unwelded

material. As a result, the probes could not make proper contact with the surface of the specimen, and no reliable reading could be obtained.

The ultimate tensile and yield strengths of the castable ODS alloys are presented in Fig. 5, and show that both measures of strength decrease dramatically after exposure to 50 dpa. The yield strengths of the ODS-1 and ODS-4 alloys decrease 50% or more after irradiation to 50 dpa, and then appear to level out. The data for the ODS-3 alloy, which are available only at 104 and 150 dpa, show that the strength of the ODS-3 alloy matches closely the strength of the ODS-1 and ODS-4 alloys. The welded ODS-1 specimens irradiated to 104 dpa and to 150 dpa both failed before reaching 0.2% strain. The specimen irradiated to 104 dpa failed in two different locations within the gage length, while the specimen irradiated to 150 dpa failed in the welded region of the gage length.

Mechanically Alloyed Cu-Cr_2O_3 and Cu-HfO_2

The two mechanically alloyed copper alloys exhibited different behavior, demonstrating the importance of the stability of the oxide used for the dispersion strengthening. Fig. 6 shows the swelling behavior of the Cu-Cr_2O_3 and the Cu-HfO_2 alloys, and clearly shows that a large difference exists. The Cu-HfO_2 alloy appears to swell slightly, although no voids were found in the specimens irradiated to 50 dpa.

The electrical conductivity of the two alloys, shown in Fig. 7, further demonstrates the difference between the two alloys. The conductivity of the Cu-HfO_2 alloy shows an unusual plateau behavior not seen in any of the other alloys. As expected, the conductivity of the Cu-Cr_2O_3 alloy continuously decreases as expected in response to swelling and transmutation.

The strength behavior of the two alloys is shown in Fig. 8. The strength of the Cu-HfO_2 alloy initially decreases but then reaches a minimum value and maintains that level throughout the rest of the irradiation. In comparison, the strength of the Cu-Cr_2O_3 alloy is lower in the unirradiated condition, and decreases steadily throughout the irradiation. Tensile curves are presented later in the report (Fig. 14) comparing the behavior of the Cu-Cr_2O_3 alloy with that of the CuAl25 alloy. Fracture surfaces for the Cu-Cr_2O_3 alloy are shown in Fig. 9, and reveal that the failure mode involved microvoid coalescence.

GlidCop™ Alloys

The GlidCop™ alloys showed the best overall swelling resistance of any of the three classes of oxide-dispersion-strengthened alloys investigated in this study. As shown in Fig. 10, the CuAl20 and CuAl25 alloys actually densify at the higher dpa levels, in contrast to the CuAl15 which swells throughout the irradiation. Swelling data for the laser-welded CuAl25 are quite variable, ranging from 19% to 43% at 104 dpa, and 8% to 20% at 150 dpa. This variability probably reflects a considerable heterogeneity in the welded zone and surrounding region.

Fig. 11 demonstrates that the electrical conductivity of the various GlidCop™ alloys exhibits essentially the same behavior despite the differing levels of cold work and Al_2O_3 content, decreasing with increasing irradiation exposure. Note that laser welding lowers the conductivity both before and after irradiation.

The ultimate tensile and yield strength of the GlidCop™ alloys are shown in Fig. 12. As observed in Cu-HfO_2, the CuAl20 and CuAl25 show the same

behavior, i.e. their strength decreases somewhat and then levels out. The strength of the GlidCop^{TM} alloys, however, is higher than that of the Cu-HfO_2 alloy both before and after irradiation, demonstrating that the only advantage to using the Cu-HfO_2 instead of the GlidCop^{TM} alloys is its surprising electrical conductivity behavior. The effect of laser welding on the strength of the CuAl25 is more dramatic compared to the castable ODS-1 alloy, primarily because of the higher initial strength of the GlidCop^{TM} alloys. The fracture surfaces for the CuAl25 alloy are shown in Fig. 13, revealing the failure mode as transgranular failure by microvoid coalescence. A comparison of the tensile curves for the CuAl25 alloy and the Cu-Cr_2O_3 alloy is presented in Fig. 14, demonstrating the dramatic differences in tensile behavior both before and after irradiation, most notably in the degree of strain hardening, total elongation, and reduction in area.

DISCUSSION

The results of this study showed that the GlidCop^{TM} alloys exhibit the best overall retention of strength, electrical conductivity, and swelling resistance, followed closely by the Cu-HfO_2 alloy which actually demonstrates the best electrical conductivity behavior for very high fluence applications. The castable ODS alloys as a group have proven undesirable due to lack of swelling resistance, a problem also encountered with the Cu-Cr_2O_3 alloy. The overall retention of electrical conductivity and strength relates directly to the resistance of the alloy to swelling, allowing the alloys studied to be divided into two groups based solely on swelling resistance. The castable ODS alloys, the laser-welded specimens, and the Cu-Cr_2O_3 alloy form one group,

whose lack of swelling resistance is comparable to that of pure copper, whereas the GlidCop™ alloys and the Cu-HfO_2 alloy demonstrate excellent swelling resistance.

In this study swelling was found to occur whenever the oxide dispersion was altered by either irradiation or laser welding. In two separate classes of alloys (GlidCops™ and castable ODS) laser welding has been shown to lead to a significant increase in swelling compared to the unwelded material. Dissolution of the Al_2O_3 dispersion in the weld zone is thought to have occurred and placed the aluminum and oxygen into solution. Both elements have been found to enhance the swelling of copper in two separate studies. Garner et al. [6,7] showed that a Cu-5Al alloy swelled more than pure copper, presumably due to the aluminum in solution. Zinkle and Lee [17] have shown significant enhancement of swelling under ion bombardment due to small concentrations of oxygen in solution. They attributed the enhancment to the oxygen stabilizing void formation by reducing the surface tension of the voids, making them more stable than dislocation loops and stacking fault tetrahedra. Other studies involving neutron irradiation of electrolytic tough pitch copper [18-20] demonstrated a swelling rate of ~2.5% dpa.

Laser welding of the CuAl25 provides a measure of just how detrimental the dissolution of the oxide can be to the electrical conductivity. Butterworth [21] reports that aluminum in solution increases the resistivity by 2.88 $\mu\Omega$ cm/wt% Al. Based on the assumption that the Al_2O_3 was completely dissolved, a preirradiation conductivity of 71% IACS (International Annealed Copper Standard) was calculated for the CuAl25 alloy compared to the measured value of 75.8% IACS. Similar calculations for the oxygen placed in solution lowers the preirradiation conductivity by an additional 3% IACS for a total

reduction to 68% IACS. The fact that the measured conductivity is somewhat higher than the calculated value suggests that most but not all of the oxide was dissolved by the laser welding process.

The poor performance of the castable ODS alloys in almost every respect provides additional information on the detrimental effect of dissolved oxygen. The alloys apparently picked up considerable oxygen during the casting process, which manifested itself as microporosity in the unirradiated base alloy, forming planar arrays of bubbles along the rolling direction of the rolled sheet [22,23]. The lower swelling of the ODS-4 alloy may be due to the higher amount of magnesium added to promote the distribution of the oxide during casting. The ODS-3 alloy contains the same amount of magnesium as the ODS-4 alloy, however. The higher swelling of the ODS-3 alloy suggests that the ZrO_2 may not be as stable under irradiation as the Al_2O_3. The poor strength of the castable ODS alloys is due in part to poor thermal stability, as demonstrated by these alloys in ageing studies [23]. This instability in conjunction with the large swelling results in very poor tensile properties.

Another mechanism whereby oxygen and aluminum may be introduced into solution is recoil resolution of the oxide particles. Spitznagel and coworkers suggested this mechanism as a possible explanation for the dissolution and amorphization of the Al_2O_3 particles observed in an ion-irradiated CuAl60 GlidCop^{IH} alloy [24]. Anderson and coworkers suggested that recoil resolution accounted for the apparent decrease in particle number density in the CuAl25 and CuAl20 alloys irradiated to 50 dpa [23]. The intensity of the oxide diffraction rings in electron diffraction patterns decreased with increasing irradiation, which led to the conclusion that the number density of the particles was smaller, and that radiation damage in the

particles perhaps altered the oxide dispersion. The densification of the CuAl25 after irradiation in this study supports the supposition that the oxide is being dissolved, and its constituents placed in solution. The relatively low swelling of the CuAl25 and the CuAl20 indicates that if the Al_2O_3 dispersion indeed undergoes recoil resolution, then the oxygen and aluminum must be recombining on a smaller scale or their effect on swelling is being counteracted somehow by the operation of another mechanism.

It may well be that the aluminum and oxygen are being reprecipitated to form smaller oxide particles. Wanderka et al. [25] presented strong evidence that in CuAl25 irradiated to 30 dpa at 293 K by 300 keV copper ions, Al_2O_3 particles smaller than 10 nm were not stable under irradiation, and that larger particles fragmented to form smaller particles. The results of their work may not be directly comparable to the present work because their study was conducted at room temperature, whereas the specimens in FFTF were irradiated to much larger fluences and at ~0.5 of the melting temperature, allowing for a stronger role of diffusion in reforming the particles.

The results of the ion irradiation study lend some credibility to the idea of recoil resolution and reprecipitation of precipitates, particularly when the irradiation temperature is fairly high and takes place over a period of several years. A recent study by Zinkle and coworkers [26] showed a 20% decrease in average particle size (10 nm to 8 nm) for the same CuAl25 alloy examined in this study after irradiation by 750 MeV protons at 470 K to 2 dpa. It is unclear whether a steady-state particle distribution had been obtained at this low dpa level [26]. Thus it is possible that irradiation to higher displacement levels may result in a greater change in particle-size distribution.

Although no microscopy results are yet available in this study to directly answer the question of recoil resolution, the tensile test results of the CuAl25 and Cu-Cr_2O_3 provide additional evidence that the oxide dispersion was altered by the neutron irradiation. Fig. 13 shows the fracture surfaces from the CuAl25 miniature tensile specimens in the unirradiated condition, and irradiated to 50 and 150 dpa. The mode of failure throughout the entire series was microvoid coalescence, accompanied by a small amount of reduction in area in the irradiated specimens. Note that oxide particles are easily visible in the dimples of the unirradiated specimen's fracture surface. They are fewer in number in the specimen irradiated to 50 dpa, however, and completely absent in the 150 dpa specimen. Whether the oxide particles have been completely dissolved or simply redistributed into very small particles that cannot be easily imaged is not apparent from the SEM micrographs. Transmission electron microscopy is in progress to answer this question.

The tensile behavior of the CuAl25, CuAl20, and Cu-HfO_2 suggests that some form of dispersoid still exists at 104-150 dpa because their high strength is maintained. The decrease in the ultimate tensile strength (UTS) and yield strength of all three alloys is attributed to recovery and recrystallization, which reduces the initial dislocation density resulting from the pre-irradiation cold work. The apparent increase in strength of the CuAl15 alloy might be a result of void strengthening, but at this point this suggestion is just speculative. The tensile curve for the CuAl25 alloy is shown in Fig. 14, and demonstrates the behavior that is representative of the CuAl20 and Cu-HfO_2 alloys as well. Of great interest is the fact that after irradiation the amount of strain hardening falls essentially to zero, with a slight drop in strength after yielding, reminiscent of a yield drop

phenomenon. The tensile curve for the unirradiated CuAl25 alloy is characteristic of a material in the 50% cold-worked state, displaying only a limited ability to strain harden due to the high dislocation density already present from the 50% cold work. The lack of any significant strain hardening in the irradiated specimens suggests that the dislocations are shearing through the particles, not bypassing them through the Orowan mechanism. Such behavior has been observed before in precipitation strengthened Al-Cu alloys [27] aged to form coherent Guiner-Preston (GP) zones. In this case the dislocations were able to cut through the GP zones, but only at a significantly higher stress than required for easy glide in either pure aluminum or solution strengthened aluminum. After irradiation, the decreasing intensity of the oxide diffraction ring, the prominent lack of particles on the 150 dpa specimen's fracture surface, and the tensile behavior of the CuAl25 all point to redistribution of the oxide to smaller particle sizes. Microscopy is in process to determine if this is actually the case, however.

The decrease in strength of the CuAl20 alloy is due to complete recrystallization after 50 dpa [23]. Anderson et al. reported that the CuAl25 alloy still retained some of its prior cold worked structure even after irradiation to 50 dpa, most likely due to the higher Al_2O_3 content. The unexpected high swelling values noted for the CuAl15 at 104 dpa represent an unexplained breakdown in the swelling resistance, perhaps due to inhomogeneous distribution of the boron and/or the Al_2O_3. The CuAl25 and CuAl20 both exhibited a reasonable amount of reduction of area even after irradiation to 150 dpa. The total elongation increased significantly after irradiation to 50 dpa, most likely due to recovery and recrystallization of the cold work induced dislocation structure. Following further irradiation to 150 dpa,

however, the total elongation decreased from ~12% to ~5%. The reason for this decrease in total elongation without swelling remains to be determined. The steady decrease in conductivity is easier to explain and is attributed to the formation of transmutation products, mainly nickel and zinc [12,13].

The strength behavior of the Cu-HfO_2 alloy following irradiation parallels that of the GlidCops™, presumably for the same reasons. The alloy was reported to be completely recovered and recrystallized after irradiation to 50 dpa [23], with the hafnia being redistributed to form smaller polygonal particles. The retention of room-temperature strength after irradiation suggests that the oxide dispersion still exists in some form to strengthen the alloy, just as in the GlidCops™. Also, the total elongation increased from 8.7% to 20.5% after irradiation to 50 dpa, and then remained constant through irradiation to 150 dpa. The reason for this behavior is not immediately obvious. The surprising electrical conductivity behavior of the Cu-HfO_2 alloy is probably caused by the transmutants and hafnia being redistributed or interacting in some manner that keeps the individual elements out of solution. One unfortunate drawback to using the Cu-HfO_2 alloy is the longer-lived radioactivity from ^{178}Hf, making it somewhat less desirable for use as a structural material.

The strength of the Cu-Cr_2O_3 alloy, shown in Fig. 8, remains roughly the same after irradiation to 50 dpa, then decreases with further irradiation. One possible explanation for the strength retention lies in the redistribution of the Cr_2O_3 particles into smaller particles. The increased degree of Orowan strengthening possibly compensates for the expected strength decrease due to complete recrystallization. The tensile curves shown in Fig. 14 for the Cr_2O_3 alloy differ drastically from the curves of the CuAl25 alloy, showing a steady

decrease in total elongation and a considerable decrease in the reduction of area.

The fracture surface of the unirradiated specimen shown in Fig. 9 contains large inclusions embedded in the surface, apparently introduced at some stage in the production of the powders. These large inclusions are no longer present at 150 dpa, presumably because they were dissolved during the irradiation. The fracture surface at 150 dpa clearly demonstrates the effect of the loss of the reduction in area, and the resultant inability to sustain even a small amount of localized deformation. The subsequent drop in strength after irradiation to 104 and 150 dpa suggests that the oxide dispersion may have coarsened during irradiation, but microscopy is needed to check this possibility. Though a gradual decrease in strength occurs, there remains a moderate amount of strain hardening, suggesting that there is still a small degree of Orowan strengthening occuring from the redistributed oxide. The higher swelling of this alloy compared to the Cu-HfO_2 and the GlidCops™ could be the result of oxygen being placed into solution by irradiation.

CONCLUSIONS

Irradiation of the several different oxide-dispersion-strengthened alloys at 415°C to 104 and 150 dpa revealed that the Al_2O_3-strengthened GlidCop™ alloys offered the best overall resistance to irradiation. A Cu-HfO_2 alloy also showed some potential despite having a higher level of longer-lived radioactivity, although pure copper becomes highly radioactive due to the formation of ^{60}Co. Both the GlidCops™ and the Cu-HfO_2 alloy exhibit similar tensile behavior, particularly with respect to the lack of strain hardening

after irradiation. Despite the apparent alteration of the oxide dispersion, the three alloys still maintain a large fraction of their strength after exposure to high fluences. The retention of electrical conductivity after irradiation of the GlidCop^{TM} alloys and the Cu-HfO_2 alloy was very good, particularly in comparison to the other alloys studied. The formation of transmutation products (Ni and Zn) is believed to be primarily responsible for the observed decrease in conductivity in the two GlidCop^{TM} alloys. An interaction between the hafnium and the transmutation products may have removed some of the transmutation products from solution, thus leading to the unusual conductivity behavior of the Cu-HfO_2 alloy. This proposal has not yet been confirmed experimentally.

The castable ODS alloys exhibited poor swelling resistance, which had a very adverse effect on their electrical conductivity and mechanical properties. The high swelling that developed in the irradiated ODS alloys appears to be the result of oxygen contamination introduced during the casting process. The swelling appeared to dominate the mechanical property behavior of the castable ODS alloys, overshadowing any possible effect that the various compositional variations of the alloys might have had in determining the strength behavior.

The Cu-Cr_2O_3 alloy exhibited relatively poor swelling resistance compared to that of the GlidCops^{TM} and the Cu-HfO_2 alloy, possibly due to the dissolution of the Cr_2O_3, which may have placed oxygen into solution. As observed in the castable ODS alloys, void swelling was primarily responsible for the poor electrical conductivity and strength of the Cu-Cr_2O_3 alloy.

REFERENCES

[1] Conn, R.W., Chuyanov, V.A., Inoue, N., and Sweetman, D.R., Scientific American, April 1992, p. 103.

[2] Vieider, G., Cardella, A., Akiba, M., Matera, R., and Watson, R., Fusion Eng. and Design, Vol. 16, 1991, pp. 23-34.

[3] Zolti, E., Fusion Eng. and Design, Vol. 16, 1991, pp. 163-171.

[4] Munz, D. and Diegele, E., Fusion Eng. and Design, Vol. 16, 1991, pp. 45-57.

[5] Akiba, M., Bolt, H., Watson, R., and Kneringer, G., and Linke, J., Fusion Eng. and Design, Vol. 16, 1991, pp. 111-125.

[6] Garner, F.A., Brager, H.R., and Anderson, K.R., J. Nucl. Mater., Vol. 179-181, 1991, p. 250.

[7] Garner, F.A. and Anderson, K.R., Fusion Reactor Materials Semiannual Progress Report DOE/ER-0313/7, 1989, p. 220.

[8] Brager, H. R., J. Nucl. Mater. 141-143, 1986, p. 79, 163.

[9] Anderson, K.R., Garner, F.A., Hamilton, M.L., and Stubbins, J.F., Fusion Reactor Materials Semiannual Progress Report DOE/ER 0313/6, 1989, p. 357.

[10] Garner, F.A., Anderson, K.R., and Shikama, T., Fusion Reactor Materials Semiannual Progress Report, DOE/ER-0313/9, 1990, p. 199.

[11] Shikama, T., Garner, F.A., Hamilton, M.L., and Anderson, K.R., Proceedings of the 15th ASTM International Symposium on Effects of Radiation on Materials, ASTM STP 1125 (in press).

[12] Garner, F.A., Heinisch, H.L., Simons, R.L., and Mann, F.M., Radiation Effects and Defects in Solids, 1990, p. 229.

[13] Garner, F.A., Hamilton, M.L., Edwards, D.J., Newkirk, J.W., Stubbins, J.F., and Mitchell, M.A., this conference.

[14] GlidCop, SCM Metal Products, Inc., 11000 Cedar Ave., Cleveland, Ohio, 44106, USA, 1988.

[15] Panayotou, N.F., Atkin, S.D., Puigh, R.J., and Chin, B.A., ASTM STP 888, 1986, p. 201.

[16] Garner, F.A., Hamilton, M.L., Heinisch, H.L., and Kumar, A.S., ASTM International Symposium on Small Test Techniques and Their Applications to Pressure Vessel Annealing and Plant Life Extension, New Orleans, Louisiana, January 29-30, 1992.

[17] Zinkle, S.J., and Lee, E.H., Met. Trans., Vol. 21A, May 1990, p. 1037.

[18] Ames, M., Kohse, G., Lee, T.S., Grant, N.J., and Harling, O.K., J. Nucl. Mater., Vol. 141-143, 1986, pp. 174-178.

[19] Lee, T.S., Hobbs, L.W., Kohse, G., Ames, M., Harling, O.K., and Grant, N.J., J. Nucl. Mater., Vol. 141-143, 1986, pp. 179-183.

[20] Harling. O.K., Grant, N.J., Kohse, G., Ames, G., Lee, T.S., and Hobbs, L.W., J. Mater. Research, Vol. 2, 1987, pp. 568-579.

[21] Butterworth, G.J., J. Nucl. Mater., Vol. 135, 1985, p. 160.

[22] Anderson, K.R., Doctoral Thesis, University of Illinois at Urbana-Champaign, 1990.

[23] Anderson, K.R., Garner, F.A., Hamilton, M.L., and Stubbins, J.F., 15th ASTM International Symposium of Effects of Radiation on Materials, ASTM STP 1125, (in press).

[24] Spitznagel, J.A., Doyle, N.J., Choyke, W.J., Greggi Jr., J.G., McGruer, J.N., and Davis, J.W., Nucl. Instr. and Meth. in Phys. Res. Vol. B16, 1986, p. 279.

[25] Wanderka, N., Yuan, Y., Jiao, L., Wahi, R. P., and Wollenberger, H., Proceedings of the 5th Inter. Conf. of Fusion Reactor Materials, held in Florida, Nov. 1991, in press.

[26] Zinkle, S.J., Horsewell, A., Singh, B.N., and Sommer, W.F., this conference.

[27] Greetham, G., and Honeycomb, R.W.K., Institute of Metals Journal,Vol. 89, 1960-1961, p. 13.

List of Figures

Figure 8 Ultimate tensile and yield strength of the mechanically alloyed Cu-Cr_2O_3 and Cu-HfO_2 alloys irradiated to 150 dpa in FFTF at 415°C.

Figure 9 Fracture surfaces of the Cu-Cr_2O_3 alloy in (a) the unirradiated condition, (b) irradiated to 50 dpa, and (c) irradiated to 150 dpa. The entire fracture surface is shown on the left, and closeup is shown on the right.

Figure 10 Swelling behavior of the GlidCop™ alloys irradiated to 150 dpa in FFTF at 415°C.

Figure 11 Electrical conductivity of the GlidCop™ alloys irradiated to 150 dpa in FFTF at 415°C.

Figure 12 Ultimate tensile and yield strength of the GlidCop™ alloys irradiated to 150 dpa in FFTF at 415°C.

Figure 13 Fracture surfaces of the CuAl25 alloy in (a) the unirradiated condition, (b) irradiated to 50 dpa, and (c) irradiated to 150 dpa. The entire fracture surface is shown on the left, and closeup is shown on the right.

Figure 14 Tensile curves of the CuAl25 alloy and the Cu-Cr_2O_3 alloy, showing the effect of neutron irradiation and the importance of the type of dispersion.

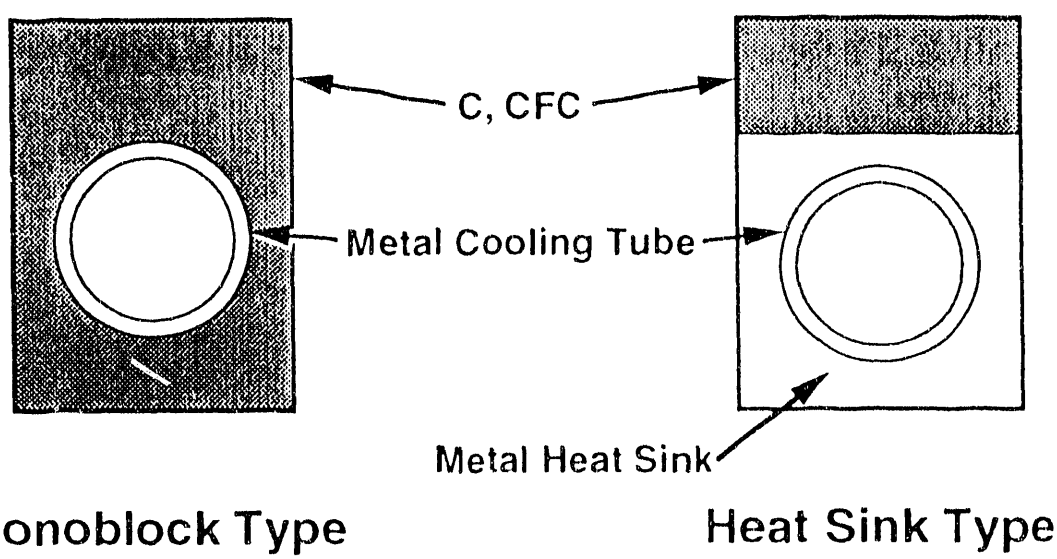

Figure 1 Two possible designs for the ITER divertor block assembly utilizing dispersion-strengthened copper alloys [ref. 1].

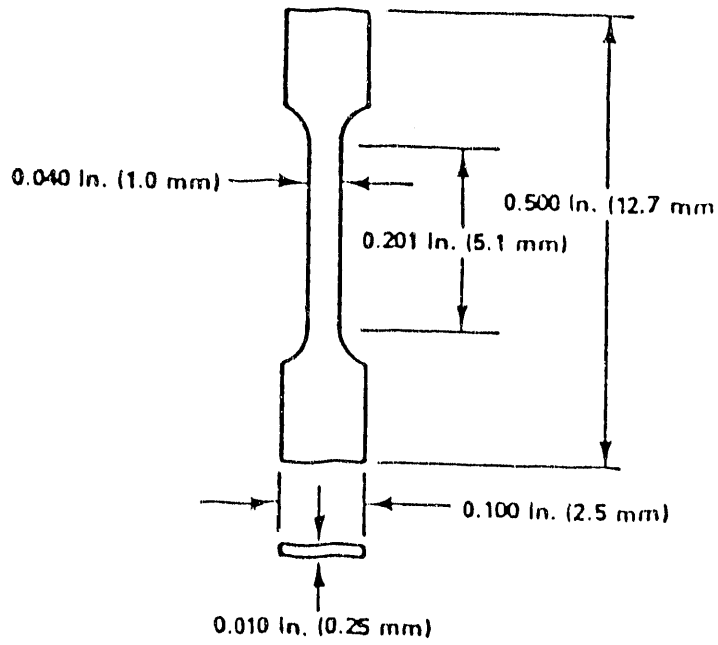

Figure 2 Dimensions of the miniature tensile specimens irradiated in FFTF.

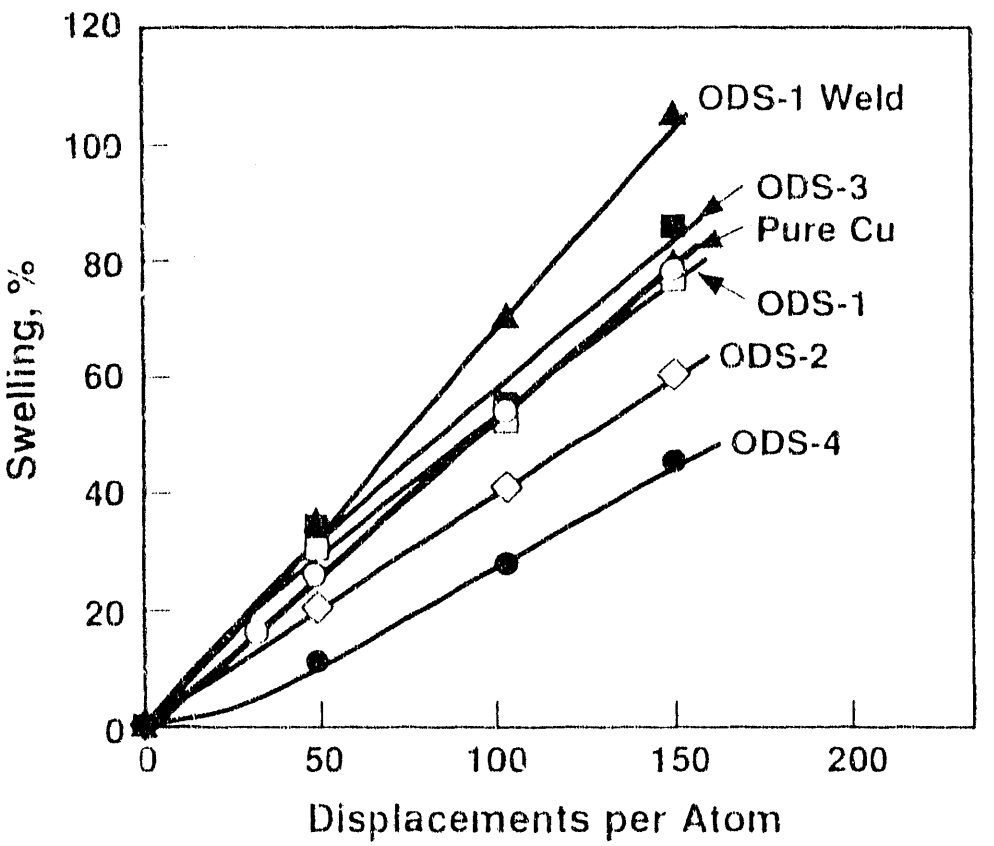

Figure 3 Swelling of the castable ODS alloys irradiated to 150 dpa in FFTF at 415°C. Swelling data for pure copper are also presented for comparison.

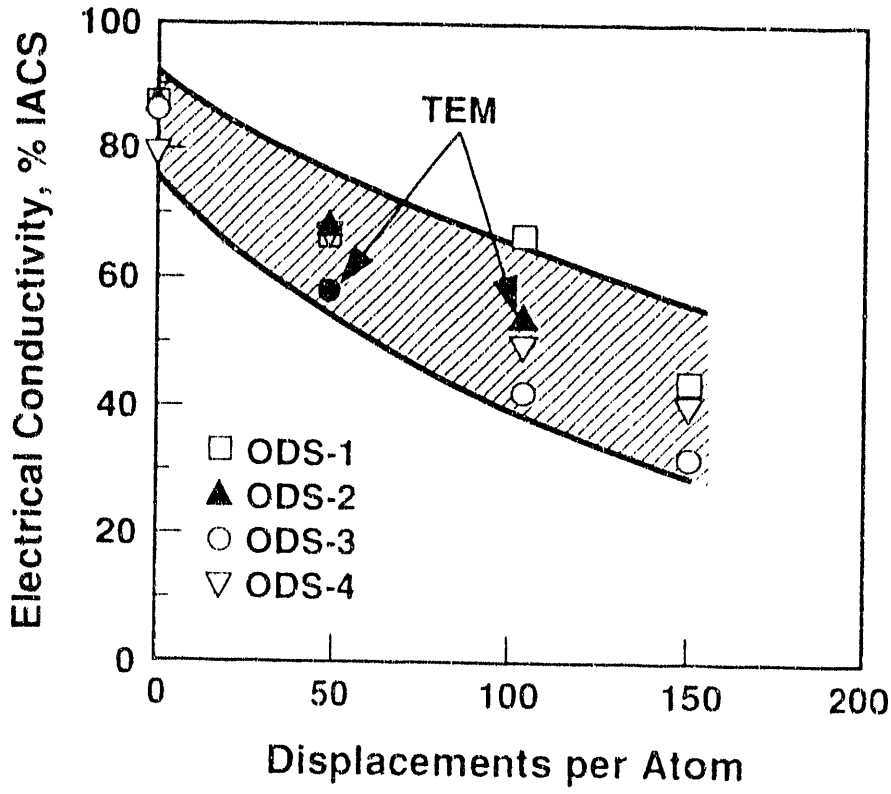

Figure 4 Electrical conductivity behavior of the castable ODS alloys after irradiation to 150 dpa at 415°C in FFTF.

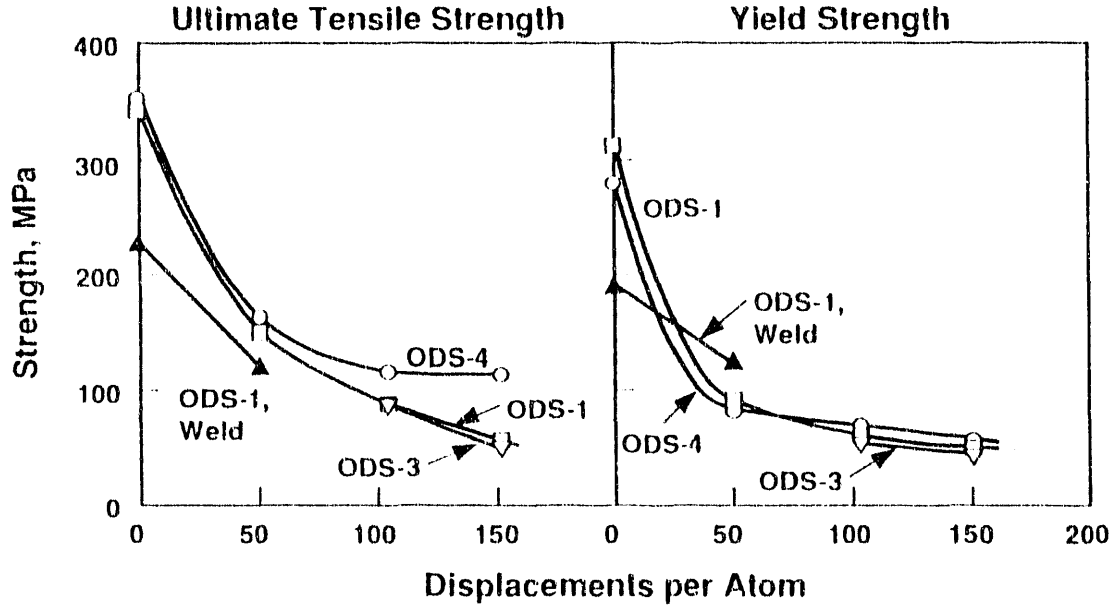

Figure 5 Ultimate tensile and yield strength of the castable ODS alloys irradiated to 150 dpa in FFTF at 415°C.

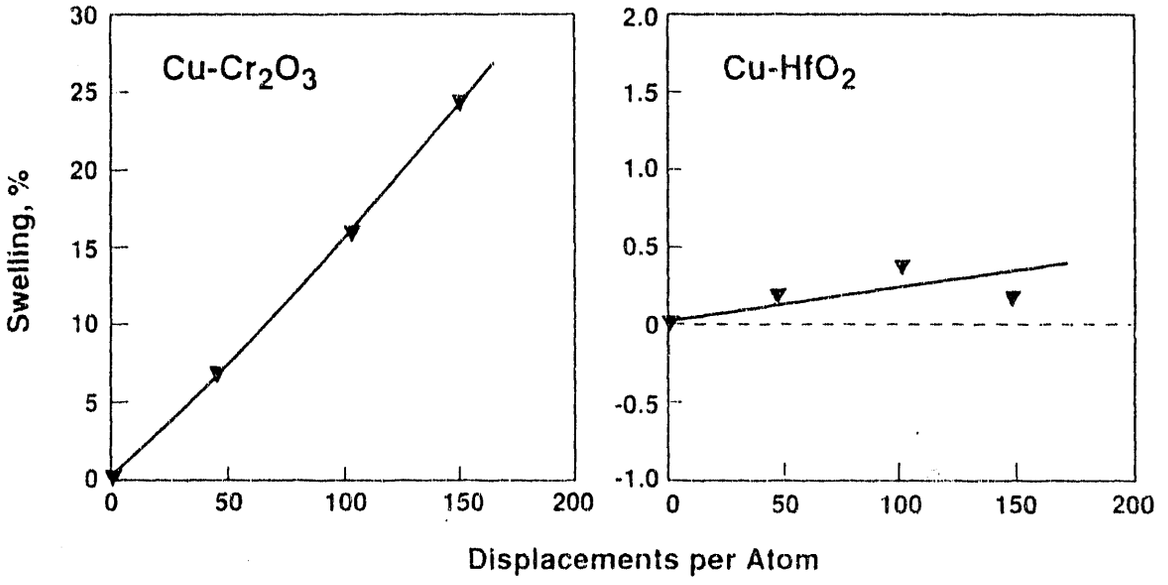

Figure 6 Swelling behavior of the mechanically alloyed Cu-Cr_2O_3 and Cu-HfO_2 alloys irradiated to 150 dpa in FFTF at 415°C.

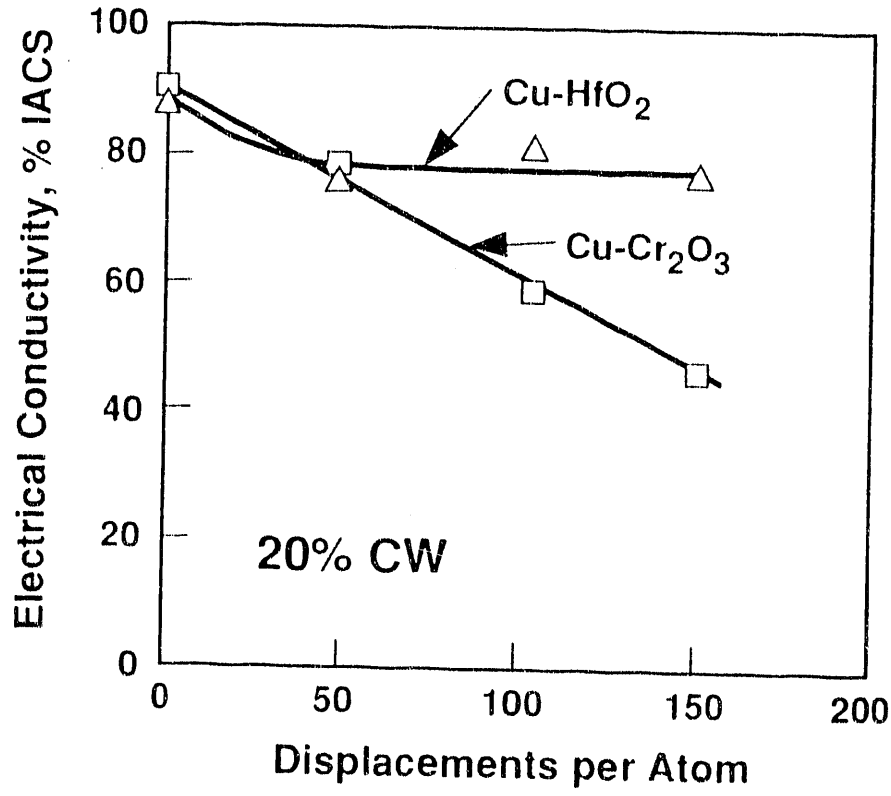

Figure 7 Electrical conductivity of the mechanically alloyed Cu-Cr_2O_3 and Cu-HfO_2 alloys irradiated to 150 dpa in FFTF at 415°C.

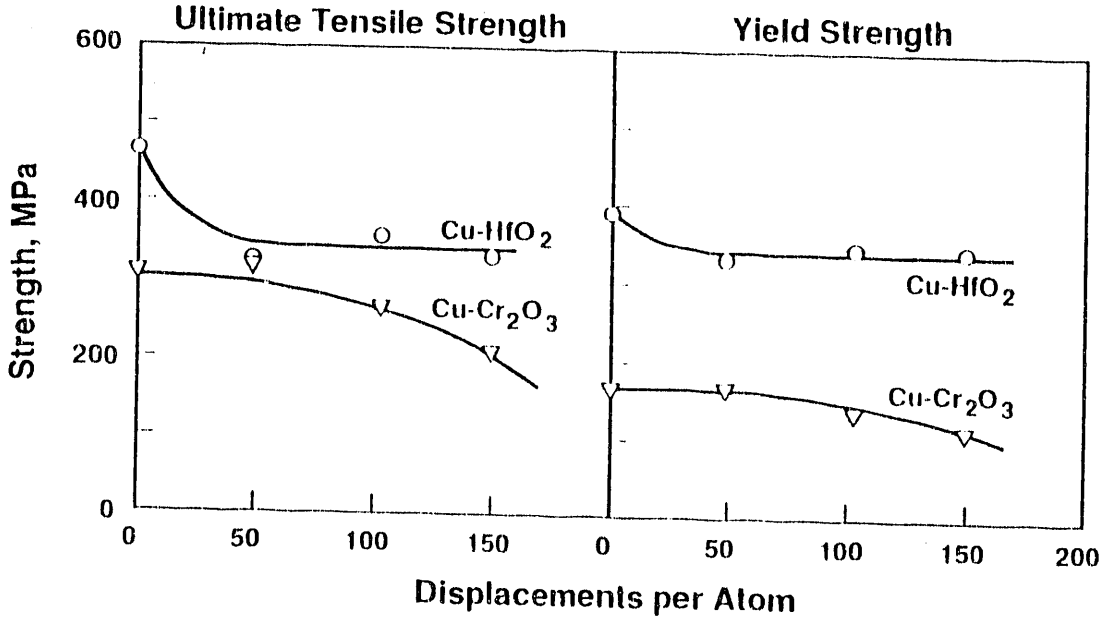

Figure 8 Ultimate tensile and yield strength of the mechanically alloyed $Cu\text{-}Cr_2O_3$ and $Cu\text{-}HfO_2$ alloys irradiated to 150 dpa in FFTF at 415°C.

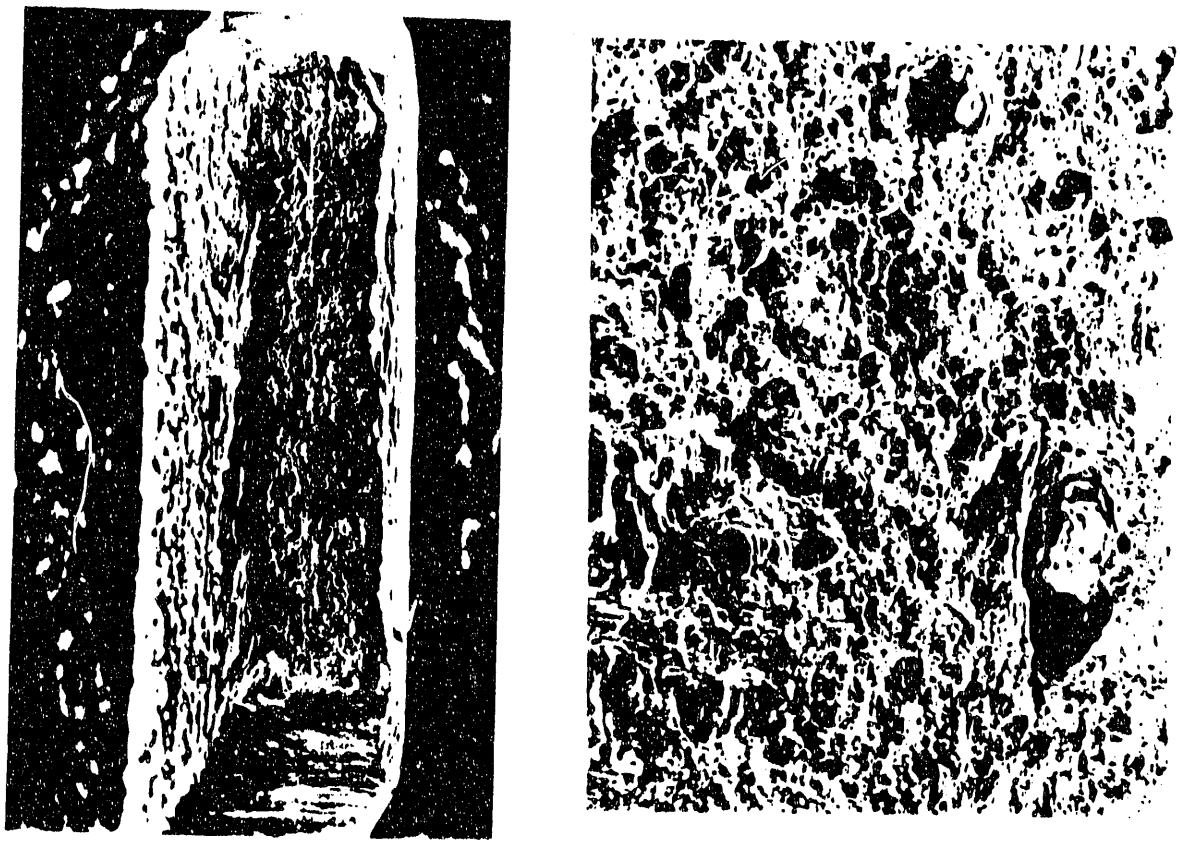

Figure 9 Fracture surfaces of the Cu-Cr_2O_3 alloy in (a) the unirradiated condition, (b) irradiated to 50 dpa, and (c) irradiated to 150 dpa. The entire fracture surface is shown on the left, and a closeup is shown on the right.

Figure 9b, $Cu\text{-}Cr_2O_3$ Irradiated to 50 dpa

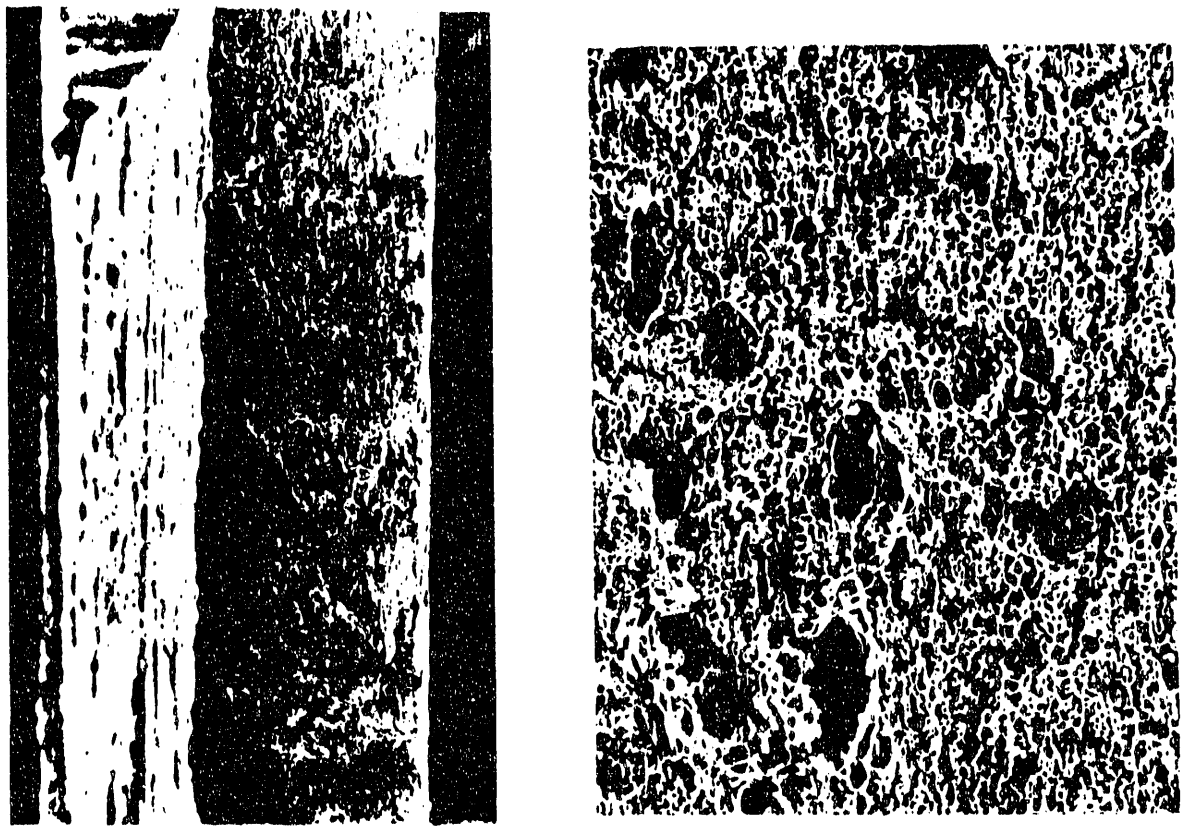

Figure 9c, Cu-Cr_2O_3 Irradiated to 150 dpa

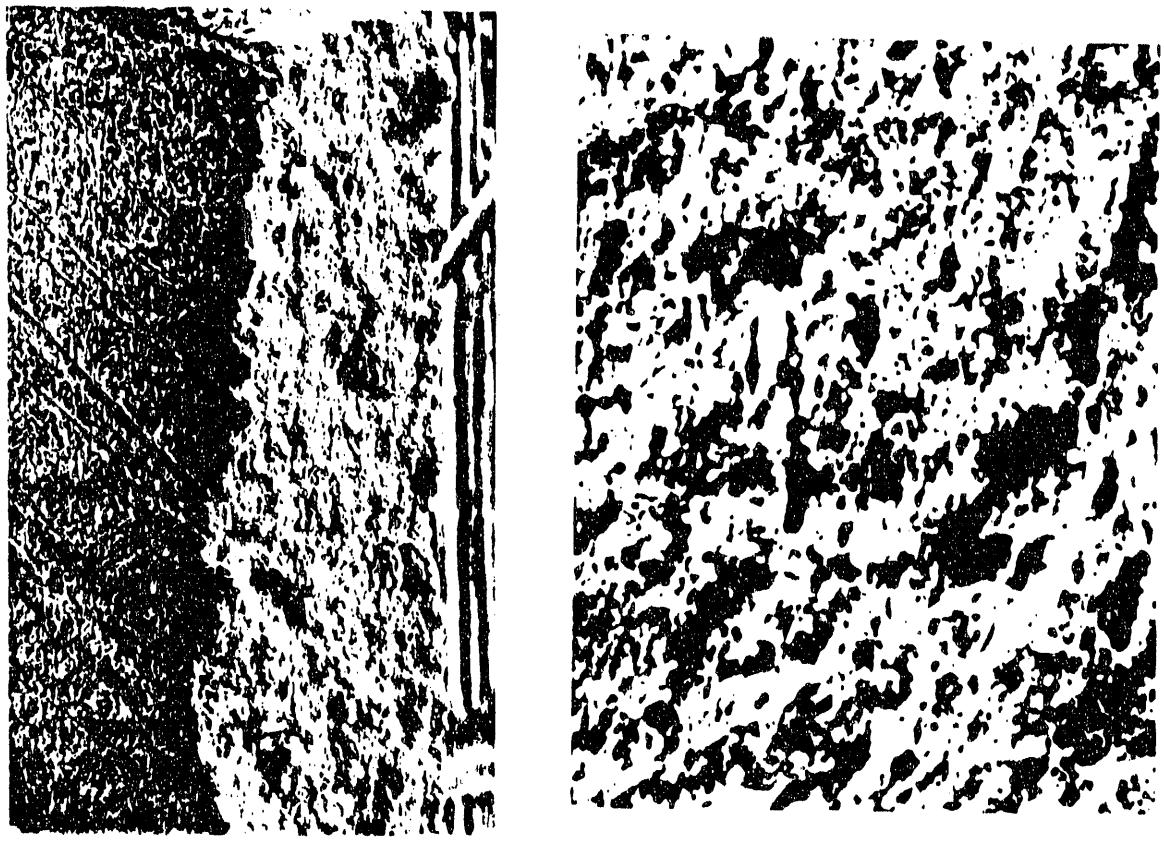

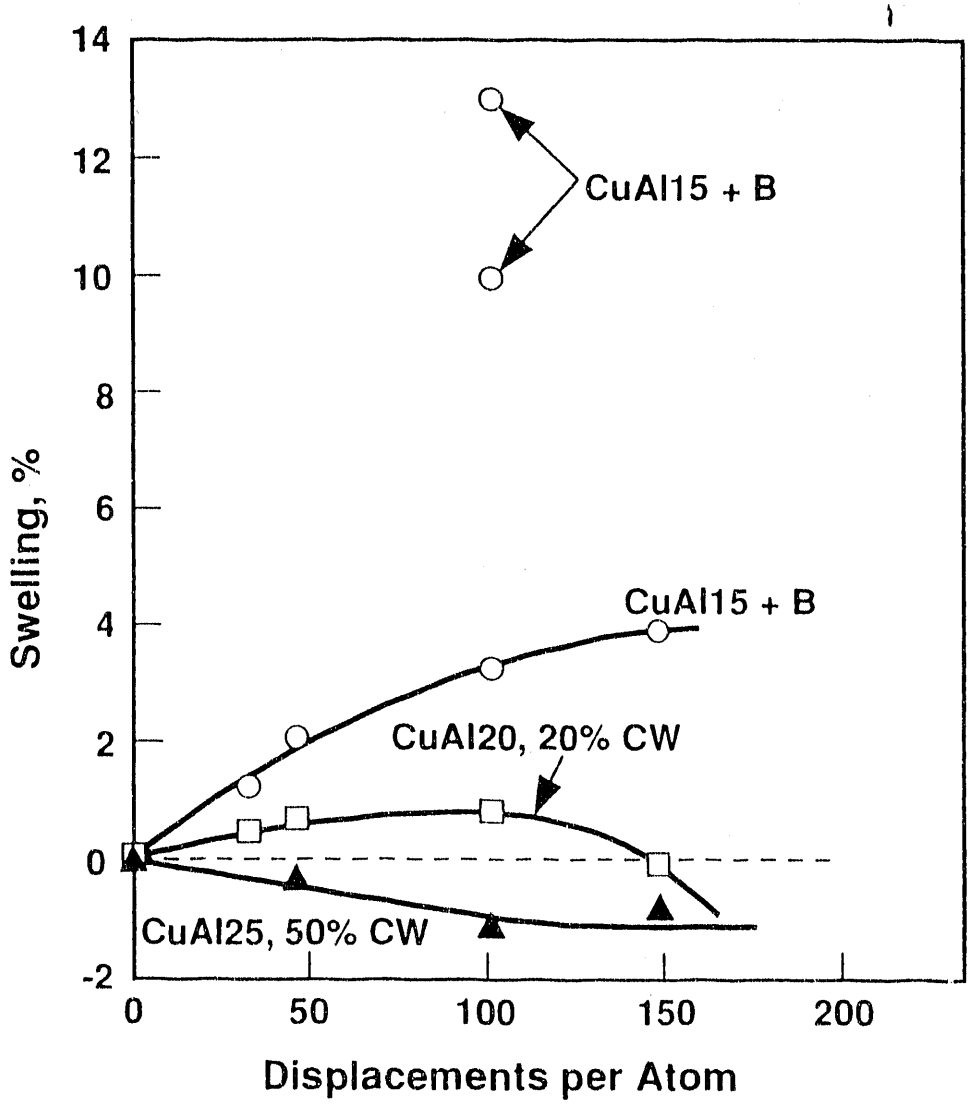

Figure 10 Swelling behavior of the GlidCop™ alloys irradiated to 150 dpa in FFTF at 415°C.

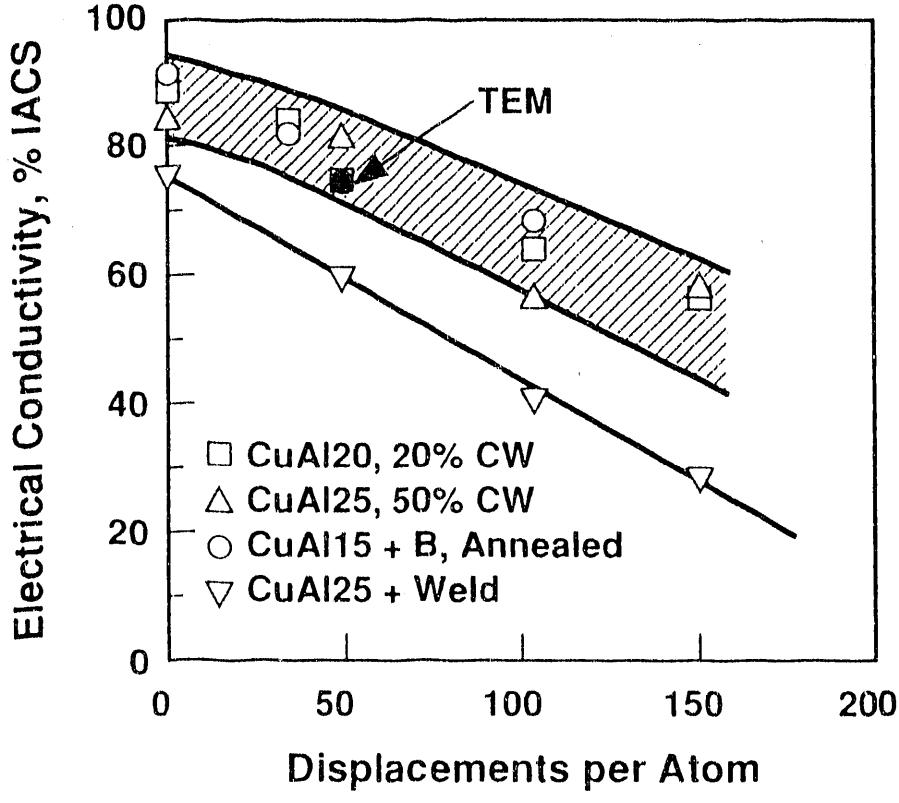

Figure 11 Electrical conductivity of the GlidCop™ alloys irradiated to 150 dpa in FFTF at 415°C.

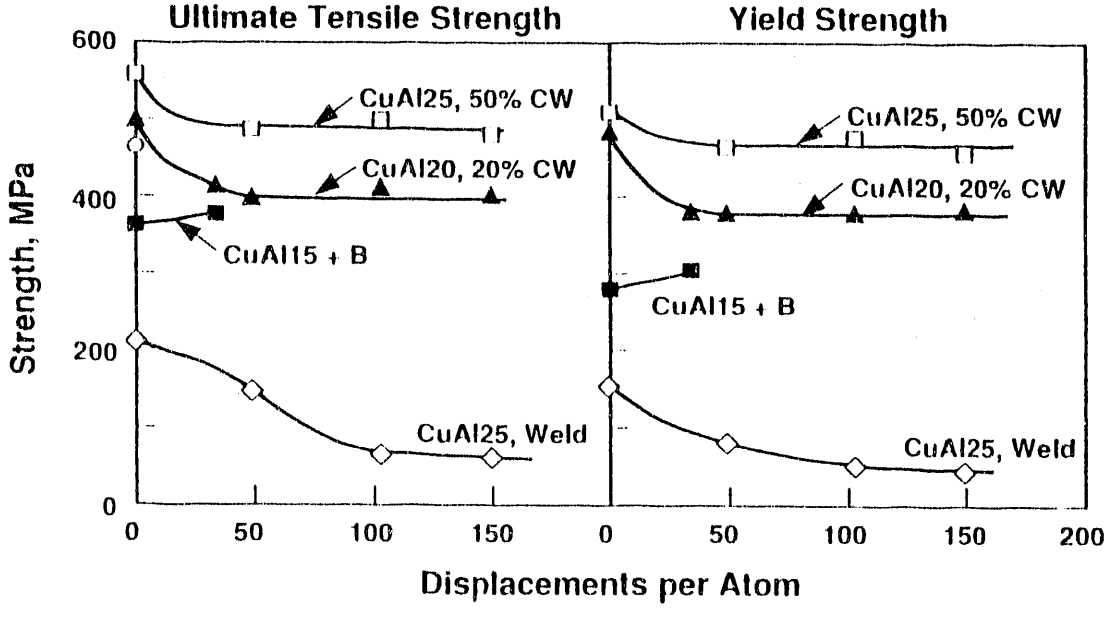

Figure 12 Ultimate tensile and yield strength of the GlidCop™ alloys irradiated to 150 dpa in FFTF at 415°C.

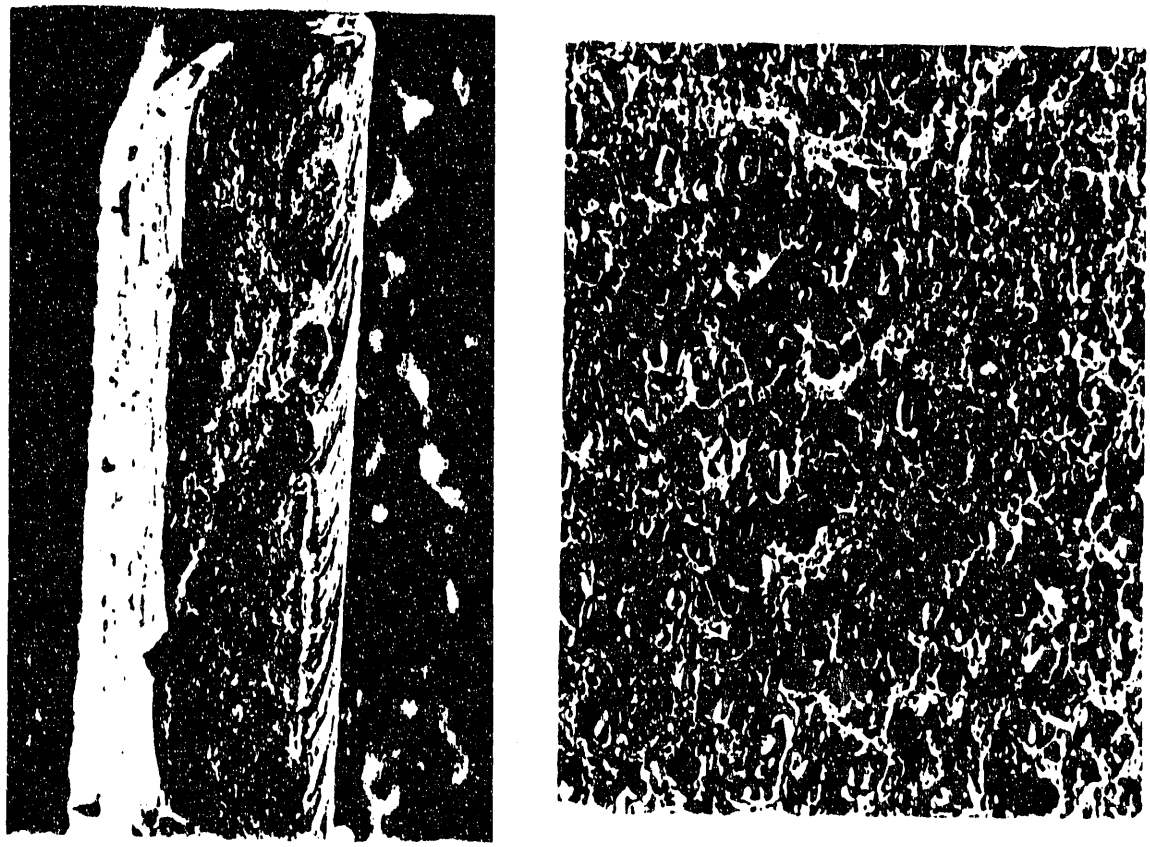

Figure 13 Fracture surfaces of the CuAl25 alloy in (a) the unirradiated condition, (b) irradiated to 50 dpa, and (c) irradiated to 150 dpa. The entire fracture surface is shown on the left, and a closeup is shown on the right.

Figure 13b, Cu-Al_2O_3 Irradiated to 50 dpa

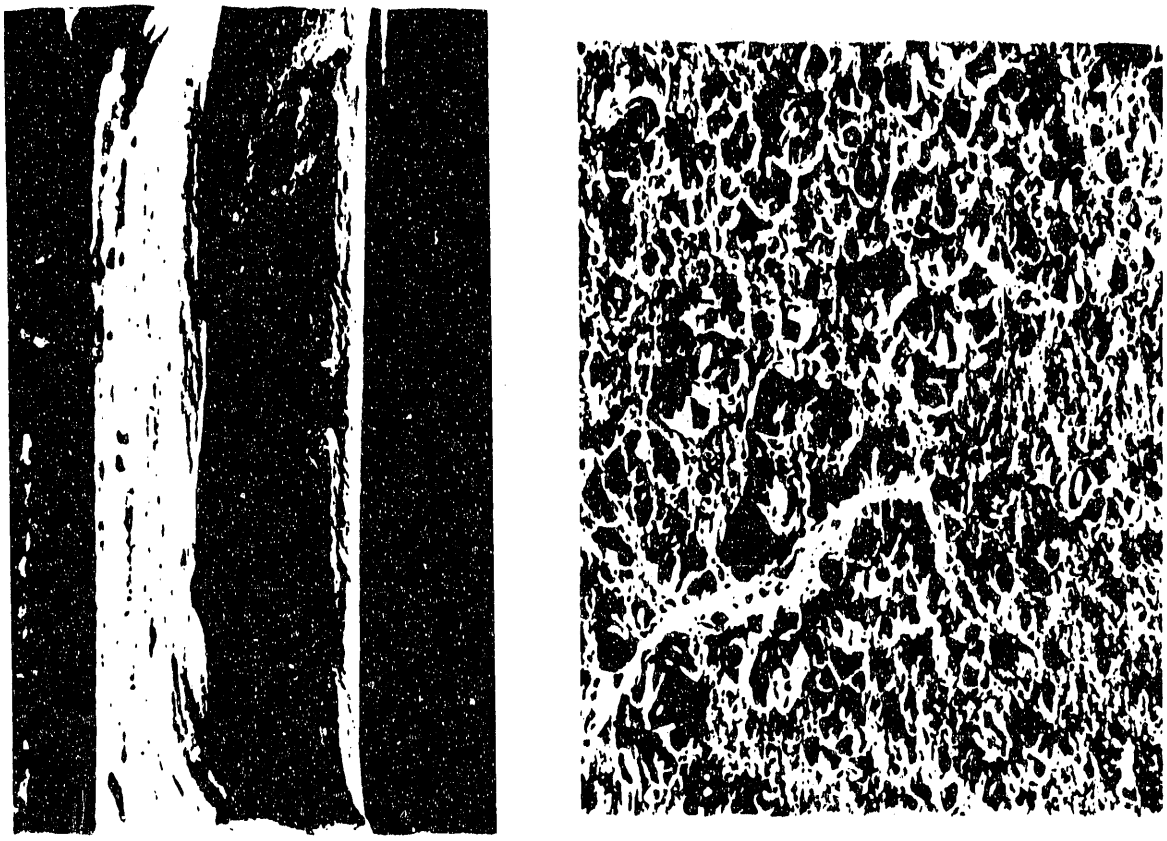

Figure 13c, $Cu\text{-}Al_2O_3$ Irradiated to 150 dpa

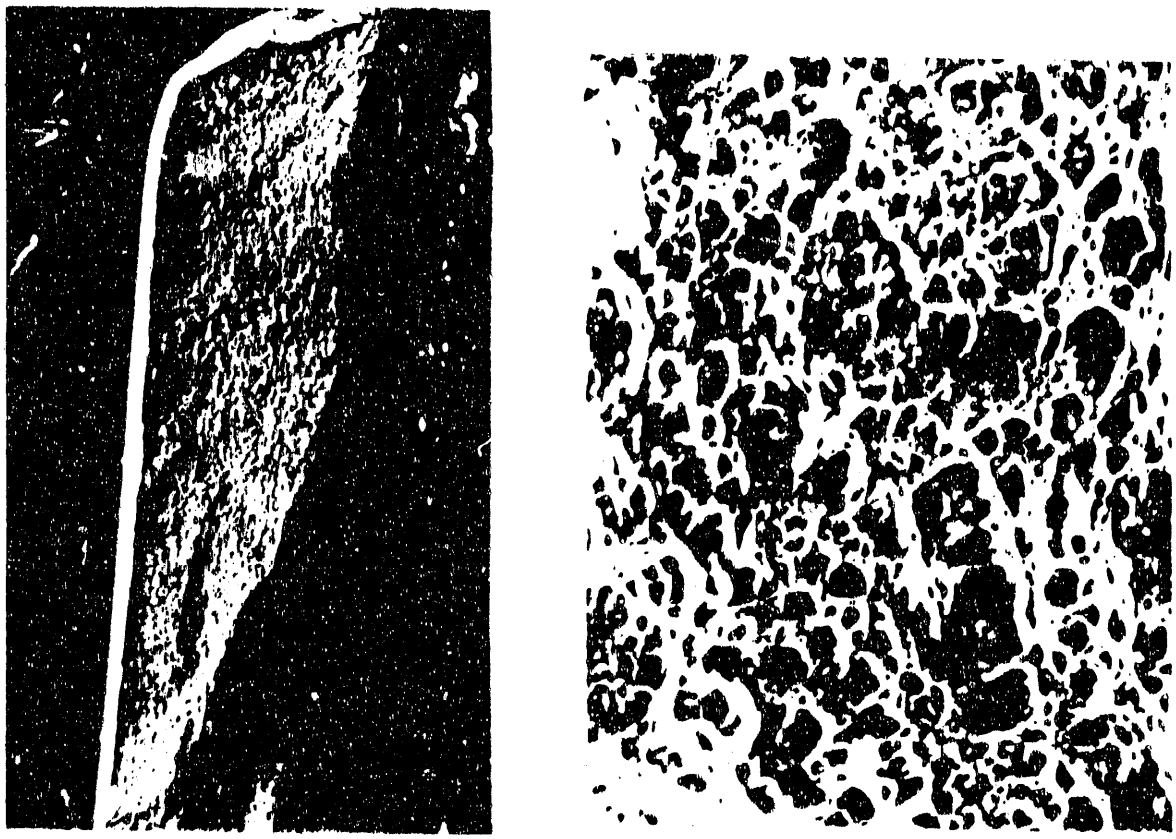

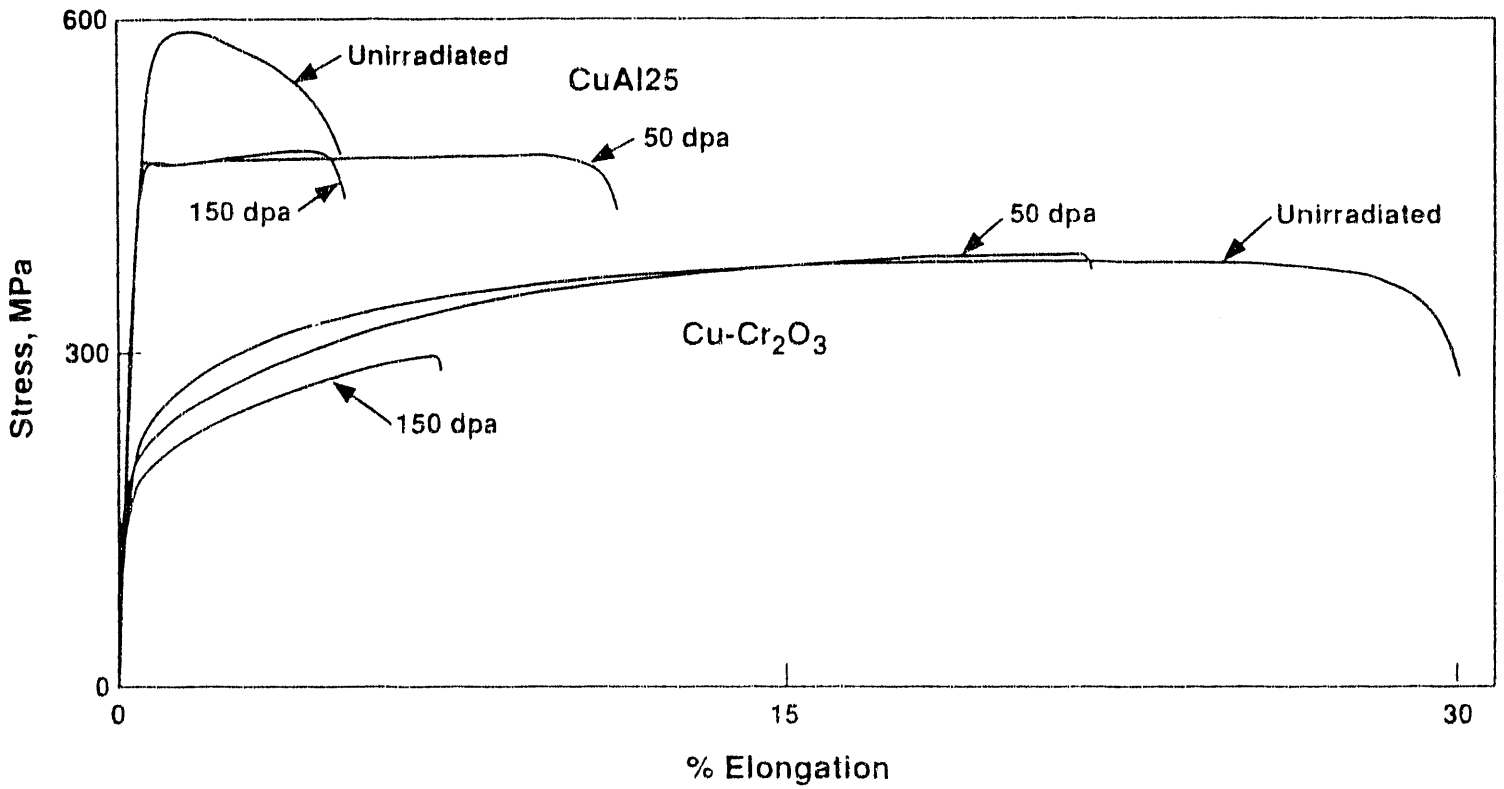

Figure 14 Typical tensile curves for the CuAl25 and Cu-Cr_2O_3 alloy, showing the effect of neutron irradiation and the importance of the type of dispersion.